LABORATORY ASTROPHYSICS USING MICROCALORIMETER AND BRAGG CRYSTAL SPECTROMETER ON AN ELECTRON BEAM ION TRAP

NASA Grant No: NAG5-5362

Progress Report 2 and 3

For Period 1 April 2003 through 31 March 2005

Principal Investigator
Dr. Eric Silver

May 2005

Prepared for:

National Aeronautics and Space Administration
Goddard Space Flight Center
Greenbelt, MD 20771

Smithsonian Institution
Astrophysical Observatory
Cambridge, Massachusetts 02138

The Smithsonian Astrophysical Observatory
is a member of the
Harvard-Smithsonian Center for Astrophysics

The NASA Technical Officer for this Grant is John Brinton, Code 810, Wallops Flight Facility; Wallops island, VA 23337

Progress Report
NASA Grant NAG5-5362

Laboratory Astrophysics using a Microcalorimeter and Bragg Crystal Spectrometer on an Electron Beam Ion Trap

For the Period April 1, 2003 to April 21,2005

Submitted by E. Silver et al.

1. Synopsis of Our Accomplishments

1.1 Instrumentation

When we last reported, we had installed a new microcalorimeter system dedicated for use on the EBIT at NIST. The instrument was checked out with its internal calibration source and EBIT plasma x-rays over several months during which time we identified several ways to further improve the performance beyond our original plans. We completed these modifications which included: 1) a redesign of the x-ray calibration source from a direct electron impact source to one that irradiates the microcalorimeter with fluorescent x-rays. The resulting calibration lines are free of bremsstrahlung background; 2) the microcalorimeter electronic circuit was significantly improved to ensure long-term stability for lengthy experimental runs [1]. A serious helium leak in the cryostat added another obstacle because it was extremely difficult to locate. It was necessary to disassemble the cryostat and return it to the manufacturer for professional repair. We are pleased and relieved to report that the system was re-assembled in early March of this year and has been operating beautifully since then.

Several photos of the new system are shown in the Appendix. The microcalorimeter spectrometer shown in Figure A1 uses liquid helium as the only expendable cryogen and it lasts for three days between refills (as opposed to every 24 hours in our earlier system which also used liquid nitrogen as a thermal shield). The new system also includes a 2-stage adiabatic demagnetization refrigerator (ADR) of novel design. As shown in Figure A2, the ADR will maintain a temperature of 60 mK for up to 51.5 hours (as opposed to 10 hours with our earlier system) with a significantly improved stability at the 3 sigma level of +/- 6 μK. The instrument includes a 4-element NTD germanium-based microcalorimeter array. The detectors routinely achieve an energy resolution of ~5 eV (in the EBIT laboratory) and under optimal conditions, 3 eV has been achieved at 6 keV [1]. This new capability is complemented in the EBIT by a radically new type of MEVVA (metal vapor arc) design that allows uninterrupted ion injection for long periods of time. It allows eight independent electrodes to be changed in vacuum with a flip of a switch, each one of which significantly outlasts a single electrode in the older MEVVA Consequently, these enhancements dramatically improve the overall efficiency of data acquisition. The spectrometer also now has the capability to synchronize photon detection with the temporal behavior of the EBIT.

1.2 Analysis

While we spent more time than expected commissioning the new instrument, a considerable effort was devoted concurrently to reconcile some of our earlier measurements of FeXVII L line emission [2] (see Section 2) with those published two years later by the EBIT group at Lawrence Livermore National Laboratory which is using a microcalorimeter built at the Goddard Space Flight Center (hereafter referred to LLNL-GSFC). The agreement between the two independent sets of

measurements is still not satisfactory. A somewhat heated debate and set of criticisms on both sides [3] has left the broader astrophysics community in a state of uncertainty about the experimental verification of the diagnostic potential of FeXVII. L emission.

2.0 Status of FeXVII as a Diagnostic For Astrophysical Plasmas

2.1 EBIT Measurements

FeXVII produces some of the strongest lines observed in astrophysical and solar x-ray observations. Six of the most important lines are labeled in Figure 1. In conditions of ionization equilibrium, FeXVII is unique in providing an important electron temperature diagnostic between two sets of these lines [4]. Its diagnostic capability, however, has been limited because the line formation mechanism is not well known and spectral modeling codes available to date have large uncertainties. In many instances the ratio of *R1=3C/3D* is frequently much lower than predicted by theory. The ratio of complete 3s to complete 3d transitions is also frequently larger than predicted by theory. This has been an ongoing challenge to theory.

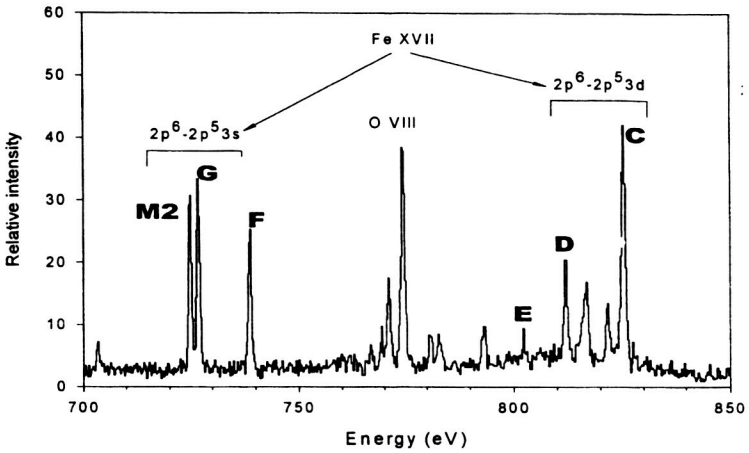

Figure 1. Selected regions from the spectrum of the active binary HR1099 made with the CHANDRA transmission grating (HETG). The FeXVII lines are denoted by their commonly used letter identifications.

In December 2000, we published the first observations of emission line intensity ratios of Fe XVII under the controlled experimental conditions of an EBIT using a microcalorimeter [2]. While we refer the reader to the publication for details of the measurements and calculations, we review some of the results here to aid in further discussion. Our results for the intensity ratio of the 15.014 line (*C* in Figure 1)) to the 15.265 line (*D* in Figure 1) are 2.94 +/- 0.18 and 2.50 +/- 0.13 at beam energies of 900 and 1250 eV, respectively. As shown in Laming et al. [2], these results are not consistent with the theoretical expectations of the collisional-radiative (CR) models which predicted the line at 15.014 Å to be stronger than what is actually observed in the laboratory, in observations by Chandra of Capella [5] and HR 1099 [6] and in spectra obtained from the sun. Prior to these laboratory measurements, the discrepancies between the theory and astronomical observations led to suggestions that resonance scattering removes photons predominantly from the line of sight in this transition [7,8,9,10,11].

The broad band capability of the microcalorimeter and its insensitivity to polarization made it possible to go beyond previous experiments with crystals; we assessed the intensity ratio of the three lines between the $2p^6$-$2p^5$3s configurations to the three lines between the $2p^6$-$2p^5$3d configurations (hereafter 3s/3d). Details may also be found in Laming et al. [2]. Two years after our first paper on FeXVII [2] was published, the LLNL-GSFC published results from their own measurements. Agreement between the two independent investigations is still not satisfactory.

2.2 Comparison of Experiment and Theory

The discrepancies among the experimental results combined with previous differences between theoretical and observational studies of FeXVII have fueled recent theoretical activity that may aid in reconciling some of the experimental controversies. The interpretation of experimental and observational ratios of line intensities has usually relied on collisional-radiative (CR) models such as those using theoretical cross-sections that neglect the fundamental role of resonant excitation. Resonant excitation preferentially affects the forbidden and intercombination transitions as opposed to dipole allowed ones. While the *3C* ($\lambda\lambda$=15.014 Å) line is dipole allowed, the *3D* ($\lambda\lambda$=15.265 Å) and *3E* ($\lambda\lambda$=15.456 Å) are spin-forbidden intercombination transitions. The majority of calculations to date has used the distorted wave (DW) approximation that neglects channel coupling and hence, resonances.

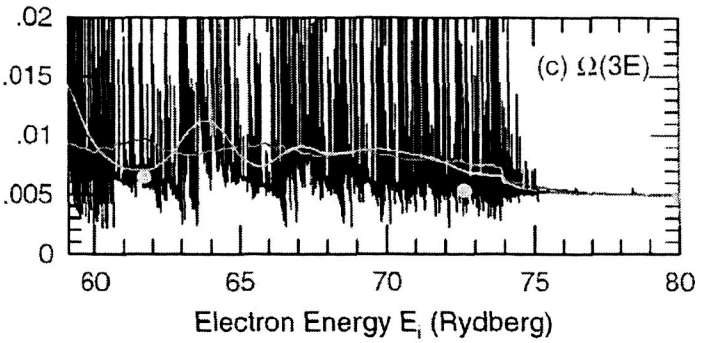

Figure 2. Breit-Pauli R-matrix collision strengths, Q, for the intercombination 3E line with resonances; the filled blue dots are distorted wave results. The Gaussina distribution (FWHM=30 eV) and numerical averages are the green and red curves, respectively (from Chen and Pradhan [40]).

Chen and Pradhan [12] have carried out what is described as possibly the largest close-coupling electron-ion scattering calculation to date (a relativistic close-coupling calculation with Hamiltonian matrix dimension up to 10,286). It predicts the existence of very narrow resonances that make the EBIT beam width appear non-negligible (indeed, relatively broad). An example of the resonance structure in the excitation collision strength is shown in Figure 2 for the *3E* (spin-forbidden) line. The blue dots are distorted wave results. The Gaussian average (GA) (FWHM = 30 eV) and numerical average (NA) are shown in green and red, respectively. Since the EBIT measurements are made at a few selected energies, the presence of resonances in the line ratios and their variation with energy *may* not be clearly discernible in a study undertaken without knowledge of these resonances.

The energy dependence of the collision cross sections predicts the relatively small differences in the *C/D* ratios in the LLNL and NIST data. They also predict that the other line ratios (3s/3d) observed by the two experimental groups can, in principle, both be achieved, assuming that different electron beam energy widths *"wash out"* the resonance structure in the excitation cross sections by different amounts.

The NIST and LLNL measurements of the *R1= 3C/3D* and *R2= 3E/3C* ratios are listed in Table 1 of Chen and Pradhan [12] which is reproduced here. Their theoretical results are also shown and are in excellent agreement with the experimental findings. We point out , however, the LLNL value for the *R1* ratio was obtained with a crystal spectrometer [4]. Microcalorimeter spectra published by LLNL [13] for the purpose of investigating other line ratios, clearly show a *R1* ratio that is not consistent with the values they published using crystal spectrometers and diffraction gratings. Since the *R1* ratio is independent of polarization corrections, the LLNL microcalorimeter measurements should agree with those of NIST/SAO. More recently, there is agreement between

the LLNL microcalorimeter and the crystal results [14].

The the 3s/3d ratios show more pronounced differences between the SAO/NIST and LLNL/GSFC EBIT results. Chen and Pradhan emphasize that the 3s/3d line ratio is not a universal

TABLE I. Comparison of the present line ratios for $R1 = 3C/3D$ and $R2 = 3E/3C$ with EBIT measurements.

		E_i = 0.85 keV	0.9 keV	1.15 keV
	EBIT	2.77 ± 0.19[a]	2.94 ± 0.18[b]	(3.15 ± 0.17, 2.93 ± 0.16)[a]
$R1 = 3C/3D$	Theory[c]: NA	2.80	3.16	3.05[g]
	Theory[c]: GA	2.95	3.27	3.10[g]
	Other theory	...	3.78,[d] 4.28,[e] 3.99[f]	...
	EBIT	...	0.10 ± 0.01[b]	...
$R2 = 3E/3C$	Theory[c]: NA	0.11	0.085	0.07[g]
	Theory[c]: GA	0.11	0.083	0.07[g]
	Other theory	...	0.04,[d] 0.05,[e] 0.05[f]	...

[a]EBIT experiments at LLNL [7]. LLNL-GSFC NIST-SAO-NRL
[b]EBIT experiments at NIST [6].
[c]Present theory with NA and GA.
[d]See Ref. [8].
[e]See Ref. [11].
[f]See Ref. [12].
[g]Present values with extrapolation of resonance enhancement from *ab initio* collision strengths from $E = 1.02$ keV (see text).

constant in an optically thin plasma excited by electron impact, but instead depends on both the characteristic electron energy (temperature) and the detailed distribution of the electron energies about that characteristic value. Figure 3 reproduced from Pradhan and Chen [15] shows this clearly. Two sets of 3s/3d ratios are plotted as a function of electron temperature. The black solid and dotted curves are produced by averaging the 89 -level CR collision strengths with a Maxwellian distribution. The solid red curve is obtained by replacing the Maxwellian with a Gaussian distribution with a FWHM=30 eV. The NIST and LLNL measurements differ most at low electron temperatures. The low energy NIST point is about as low as the LLNL point is high compared to the 30 eV Gaussian distribution. The NIST value at 1.24 keV agrees quite well with the Gaussian distribution model while the LLNL data is high. We

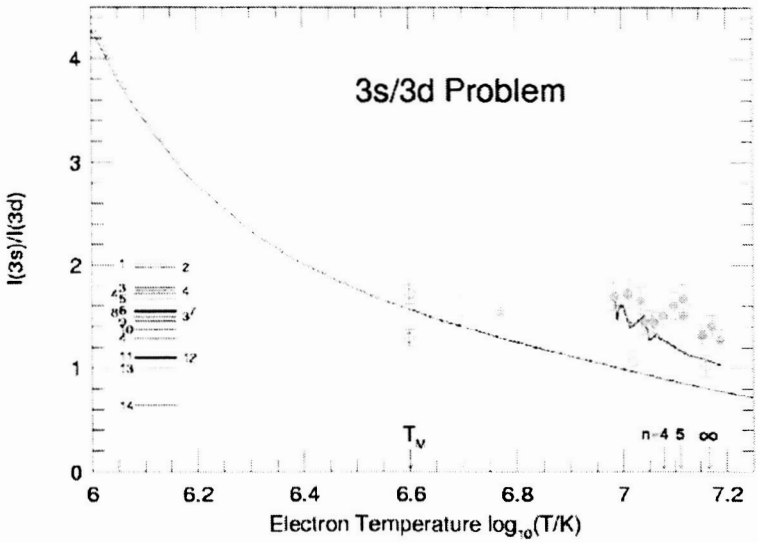

Figure 3. Theoretical x-ray line ratios vs electron temperature compared with observations from solar corona of Capella at 5-6 x ^{106K} from Chandra (open blue circle and XMM-Newton (filled blue circle, from the solar corona at Tm = 4 x 10^6 K(open red circles and from LNL and NIST EBIT experiments(filled and open green circles, respecively). The scattered data labeled 1-15 are for various types of observated values from solar, stellar and disk corona (see details in Chen and Pradhan [15]).

point out that if the resonance theory is correct, it is also quite reasonable to expect the red curve to show a more distinct dip near the low energy of the NIST data when the calculation is redone in finer energy steps. We point out that the open red circles represent the 3s/3d ratios for the solar corona. The blue circles (open and closed) are for Capella observed with CHANDRA and XMM-Newton.

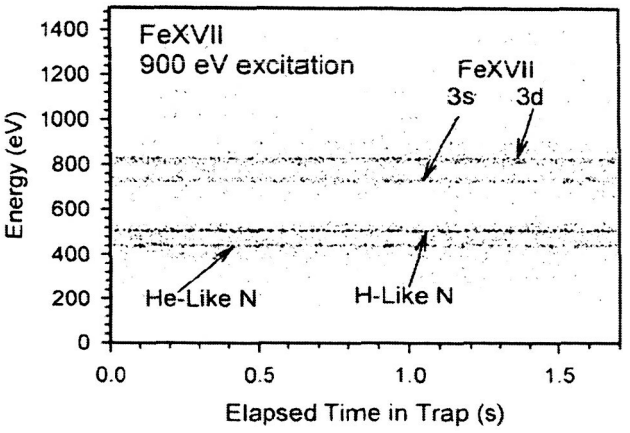

Figure 4. Event-mode spectra showing the temporal evolution of the emission lines following MEVVA injection of Fe. The plot shows conclusively that the only ionic species from Fe are those from FeXVII (top pair of lines). The bottom pair of lines are those from He-like and H-like nitrogen which is the cooling gas used in these experiments.

Accurate measurements of beam widths are crucial. The electron distribution function (EDF) in turn, bears on physical effects such as space charge potential, beam currents, polarization corrections, etc. Nevertheless, the theoretical sets of 3s/3d ratios clearly demonstrate that they are sensitive to the plasma conditions, i.e., these are *source-specific*. By the same token, the theoretical results will also need to be extended to other electron distribution functions (EDF) to elicit a more complete description of resulting variations in line intensities.

Independent of the astrophysical observations, we can say that while some of the line ratios measured in the LLNL experiment are in relatively good agreement with our results, other ratios disagree at the 2-sigma to 3-sigma level. (Note that the "typical" error bars in Figure 3, provided by Chen, do not precisely correspond to the published values for all energies; in specific, the error bar on the LLNL data just above our low energy data point at 900 eV should be much larger). LLNL suggests that charge contamination in the NIST EBIT is the cause for the lower SAO-NIST-NRL values, especially at 900 eV. We can only rule this out by collecting time-dependent (*event-mode*) spectra, a technique that in earlier work we did not employ. In our new system, *we can* produce event-mode spectra. Figure 4 is an example of event-mode plot showing the temporal evolution of the emission lines following the MEVVA injection of iron. Injection occurs at zero time. The plasma emission lasts for 1.7 sec at which time the MEVVA fires again. The only ionic species in the plasma are he-like and hydrogen-like nitrogen and the FeXVII complex of lines verifying that the FeXVII lines are not contaminated by other ionic species. The associated spectrum produced from this event-mode data is shown in

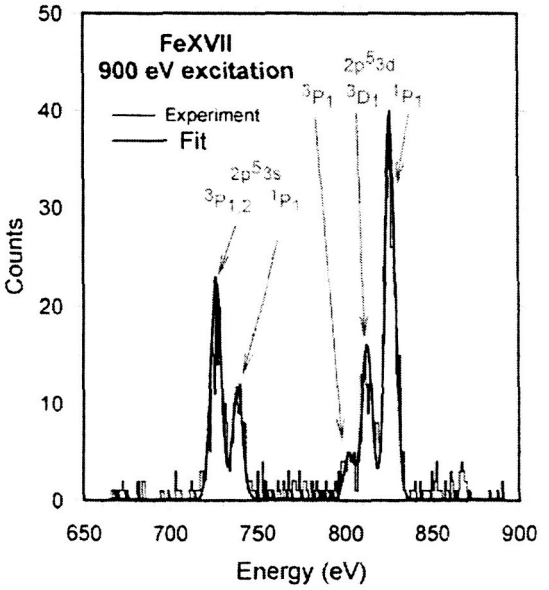

Figure 5. The spectrum produced from the event-mode data in Figure 4. Only the FeXVII lines are shown. This data was recently obtained with the new microcalorimeter and has better resolution than the data we previously published in Laming et al [2].

Figure 5 where we have isolated the FeXVII emission between 700 eV and 900 eV. We point out that this spectrum was obtained just recently with one of the four detectors in our new microcalorimeter system. It has not been corrected for the window transmission. Its energy resolution is about 5 eV which is better than our previously published result [2]. We point out that LLNL-GSFC was only able to demonstrate that line intensity contamination occurred when gas-phase Fe injection was employed, a method known to produce high levels of charge state contamination.. At NIST, a MEVVA (metal vapor arc) is used to inject Fe .

References

1. E. Silver et al., *Nucl. Instr. and Meth. in Physics Research(Section A)* (2005) in press.
2. M. Laming et al., *Ap.J.*, **545**, L161(2000)
3. Gillaspy et al.,Published in CP730, *Atomic Processes in Plasmas: 14th APS Topical Conference on Atomic Processes in Plasmas* edited by J. S. Cohen, S.Mazevet, and D. P. Kilcrease, (AIP, New York, 2004) p. 245-254. (2004)
4. Brown,G.V., et , *Ap. J.* , **502**,1015 (1998)
5. Brinkman, A. C., et al. (2000), *ApJ*, **530**, L111
6. Available through the *NASA Emission Line Project*. (1999).
7. Schmelz, J. T., Saba, J. L. R., & Strong, K. T., *ApJ*, **398**, L115 (1992)
8. Phillips, K. J. H., Greer, C. J., Bhatia, A. K., & Keenan, F. P., *ApJ*, **469**, L57 (1996)
9. Phillips, K. J. H., et al., A&A, **324**, 381 (1997)
10. Bhatia, A. K., & Doschek, G. A. (2000) private communication
11.Saba, J. L. R., Schmelz, J. T., Bhatia, A. K., & Strong, K. T. *ApJ*, **510**,1064 (1999),
12. Chen, G., and Pradhan, A., *Phys. Rev. Lett.*, 89, 1,(2002)
13. Beiersdorfer et al., Ap. J. Lett., 576,L169 (2002)
14.Brown, G, to be published in the proceedings of *X-ray Diagnostics for Astrophysical Plasmas: Theory, Experiment, and Observation* (2005)
15. Chen, G., and Pradhan, preprint, submited to *Phys Rev A*(2002)

Talks and Papers For This Reporting Period

1. Gillaspy et al.,Published in CP730, *Atomic Processes in Plasmas: 14th APS Topical Conference on Atomic Processes in Plasmas* edited by J. S. Cohen, S.Mazevet, and D. P. Kilcrease, (AIP, New York, 2004) p. 245-254. (2004)

2. Tan et al., in the *Proceedings of the 8th International Colloquium on Atomic Spectra and Oscillator Strengths,* to be published in **Physica Scripta T**, co-edited by James Lawler, Glenn Wahlgren and Wolfgang Wiese, University of Wisconsin, Madison, Wisconsin, 7-12 August 2004.

APPENDIX

Commissioning the New SAO/NIST Microcalorimeter On The EBIT

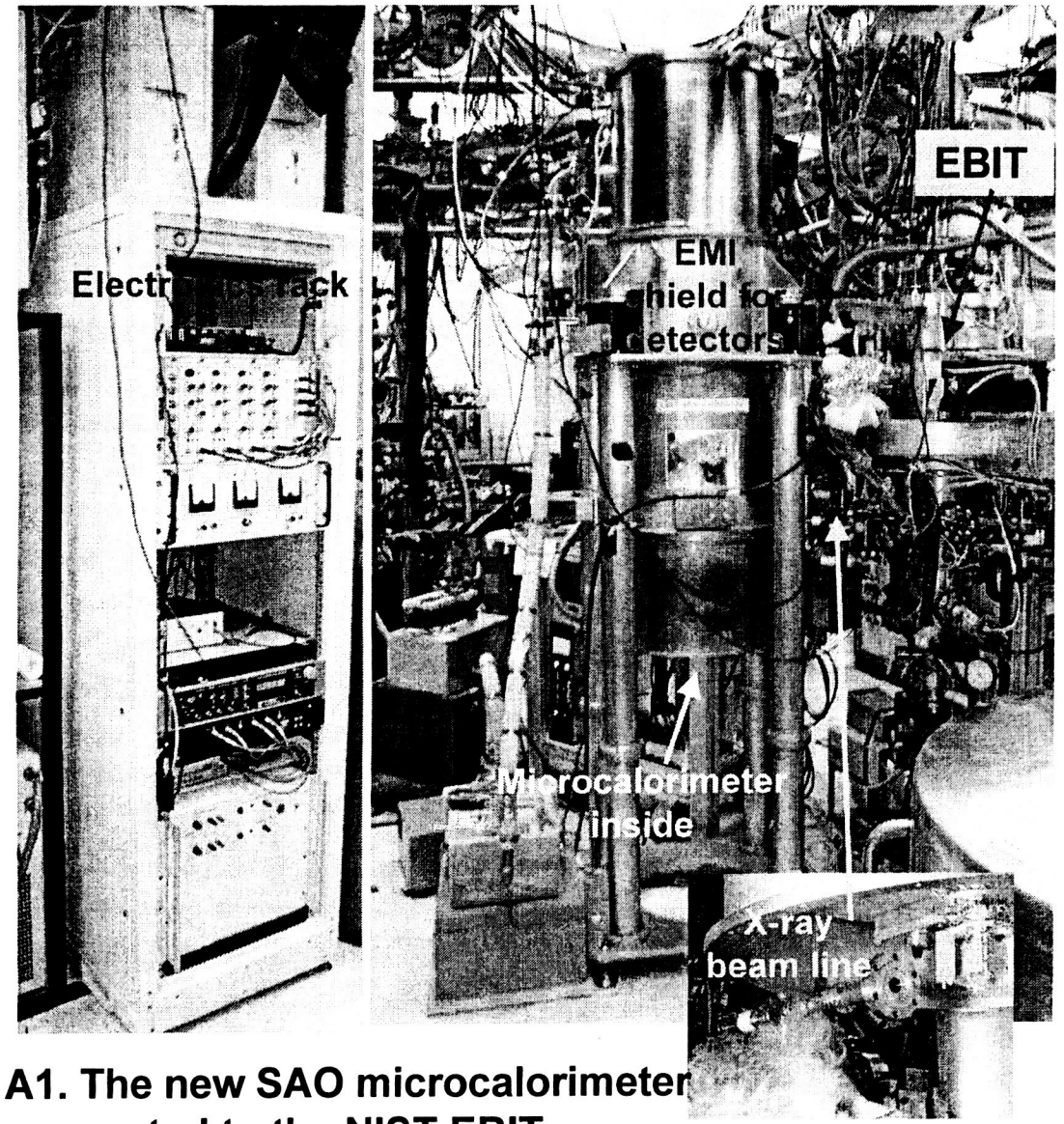

- 1 x 4 pixel NTD Ge array
- 2-stage ADR
- 72 hour hold time for LHe^4
- 51 hour hold time at 60mK
- Built-in x-ray tube for calibration

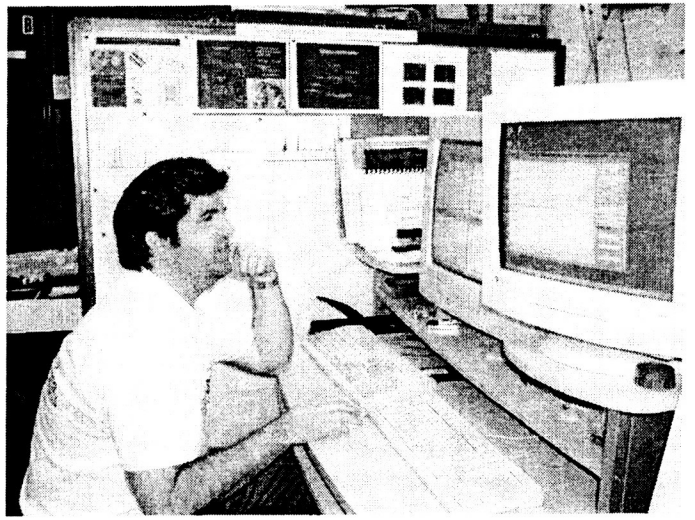

A1. The new SAO microcalorimeter connected to the NIST EBIT.

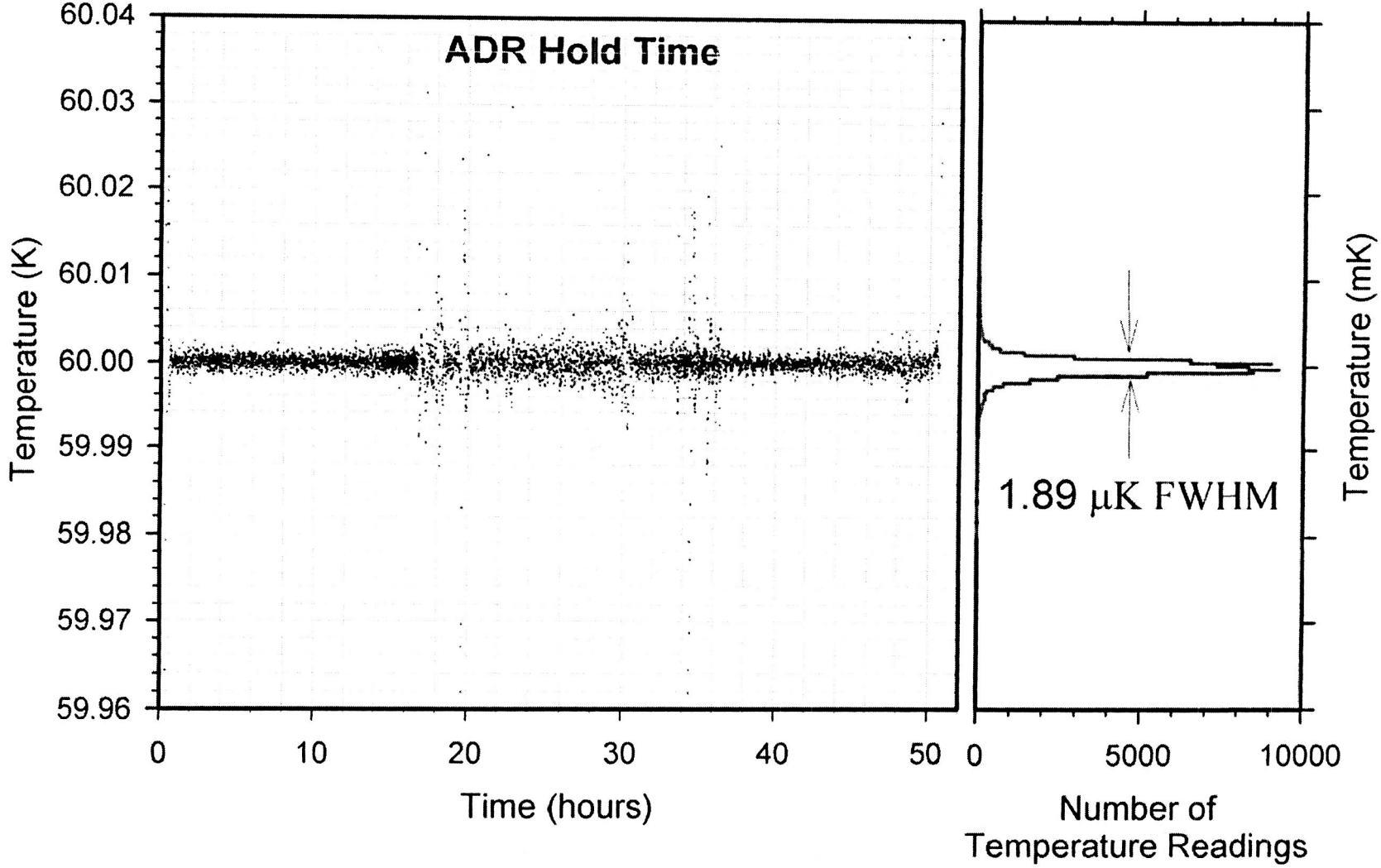

A2. (Left) A record of the detector temperature as a function of time. (Right) The distribution of the temperature readings. The stability at the 3 sigma level is +/- 6 μK , more than sufficient to achieve the energy resolution performance.